Postprint of the article published in:
Journal of Crystal Growth 360: 123-126 (2012)
doi: 10.1016/j.jcrysgro.2011.12.032

Processing, microstructure and optical properties of the directionally solidified Al_2O_3-$EuAlO_3$ eutectic rods

P. B. Oliete*, M. C. Mesa, R. I. Merino and V. M. Orera

Instituto de Ciencia de Materiales de Aragón (ICMA), CSIC-Universidad de Zaragoza

C/ María de Luna 3, 50018 Zaragoza, Spain

Revised manuscript 28 November 2011

* Corresponding author: P. B. Oliete Tel: +34 976 761 958; Fax: +34 976 761 957

e-mail addresses: poliete@unizar.es (P.B. Oliete); mcmesa@unizar.es (M. C. Mesa); rmerino@unizar.es (R. I.Merino); orera@unizar.es (V. M. Orera)

ABSTRACT

Al_2O_3-$EuAlO_3$ eutectic rods were directionally solidified using the Laser-Heated Floating Zone method, also known as Laser-Heated Pedestal Growth technique, with growth rates ranging between 25 and 750 mm/h. The microstructure was found to be highly dependent on the processing parameters, the size of the phases decreasing with the growth rate down 200 nm in samples grown at 750 mm/h. At low rates, an interpenetrated network of the eutectic phases was obtained whereas at high growth rates a tendency towards a nanofibrous pattern was observed. The optical absorption and photoluminescence of the eutectics grown at 100 mm/h and 350 mm/h were measured at room temperature. The Judd-Ofelt parameters, Ω_2, Ω_4 and Ω_6, were obtained from the absorption spectra. Under a 396 nm lamp excitation, a red light emission centred in 616 nm corresponding to the Eu^{3+} ion was detected. The Eu^{3+} emission was stronger in the samples with the finer microstructure.

Keywords: A1. Eutectics; A1. Luminescence; A2. Floating zone technique; B1. Europium compounds; B1. Al_2O_3-$EuAlO_3$; B2. Phosphors

1. INTRODUCTION

Large investigation efforts have been devoted to directionally solidified ceramic eutectics due to their interesting properties, which result from being composites fabricated in situ with fine microstructures controlled by the solidification parameters [1]. Among them, those based in Al_2O_3 outstand by their microstructural stability and mechanical behaviour up to temperatures near the melting point [2-4]. In addition to their excellent performance as structural material, the unique features of the eutectic microstructure allow to extend the use of these materials to functional aplications. For instance, the contrast in the refractive index between the constituent phases allows to produce efficient light guiding in some eutectic ceramics [5]. The functional application field of these materials can be extended with the addition of rare earths (RE) to the eutectic system. In particular, the lifetime of the Er^{3+} luminescence at 1.5 μm in Al_2O_3-ZrO_2 Er-doped directionally solidified eutectics has been shown to be modified by changes in the size of the microstructure [6]. More recently, Al_2O_3-$Er_3Al_5O_{12}$ eutectic ceramics have been investigated as selective emitters for a thermophotovoltaic generation system [7]. In the optical field, Eu^{3+} ion stands out due

to their interesting luminescence properties. We should note that the incorporation of europium to a large variety of materials have been investigated as potential phosphors [8-9], as Eu^{3+} can be used like a red light source because of its strong red emission when exciting with UV light.

In this work, directionally solidified Al_2O_3-$EuAlO_3$ eutectic rods were studied. Up to our knowledge, only two preliminary studies in Al_2O_3-$EuAlO_3$ eutectics have been reported [10, 11]. In [10] the material was grown using a very low solidification rate and presented a rather coarser microstructure than that studied here. Reference [11] corresponds to a eutectic phase identification study in different Al_2O_3-RE_2O_3 systems grown by the micro-pulling-down method. X-Ray diffraction in Al_2O_3/Eu_2O_3 system allowed to identify the eutectic phases as α-Al_2O_3 and $EuAlO_3$.

The aim of this work is to study the microstructure and optical properties of the Eu^{3+} ion in the Al_2O_3-$EuAlO_3$ eutectic ceramic. The eutectic rods were fabricated in a large range of growth rates up to 750 mm/h in order to investigate the effect of the processing parameters on the microstructure and the Eu^{3+} emission. The ceramic eutectics were processed by the Laser-Heated Floating Zone method (LHFZ), also known as Laser-Heated Pedestal Growth technique. LHFZ method presents important advantages as no crucible is needed, avoiding contamination of the samples, the growth atmosphere can be modified and large axial thermal gradients at the solid/liquid interface are achieved which allows obtaining homogeneous eutectic microstructures even when high solidification rates are used [1]. The main goal of the investigation was the eutectic microstructure control in phase size and morphology using the solidification rate as the control parameter. The use of high growth rates produced a refinement of the microstructure and a stronger Eu^{3+} emission in the Al_2O_3-$EuAlO_3$ eutectic ceramic.

2. EXPERIMENTAL DETAILS

Ceramic rods of the system Al_2O_3-Eu_2O_3 with the reported eutectic composition (76% mol Al_2O_3 and 24% mol Eu_2O_3) [12] were processed by the LHFZ method at solidification rates ranging between 25 and 750 mm/h in order to obtain different microstructures. A CO_2 laser was used as the heating source. The rods were solidified in air except the sample grown at the highest growth rate, which was processed in nitrogen in order to avoid gas inclusions in the rod during solidification. Previous

studies of the effect of changing the growth atmosphere in other Al_2O_3-based eutectics conclude that the voids in rods grown at high pulling rates are highly reduced using a nitrogen atmosphere [13]. However, no effect of the growth atmosphere was observed in the microstructure and no different phases were found in the eutectics.

Cylindrical ceramic precursors (feed rods) of 2-2.5 diameter and 10 cm length were obtained from cold isostatic pressing. Up to two densification steps were performed previous to the final growth to reduce the precursor porosity. These steps consisted of LHFZ growths at solidification rates between 100 and 250 mm/h performed in the atmosphere used for the final crystal growth. Last stage was always performed with the solidified rod being pulled out downwards and without rotation of the crystal and precursor using the corresponding solidification rate (25-750 mm/h). Directional solidified rods with typical diameters of 1-1.5 mm were obtained.

The microstructure was studied for the different growth rates. Polished transverse and longitudinal cross-sections were observed using Scanning Electron Microscopy (SEM) (model 6400, Jeol, Tokyo, Japan). The phases present in the eutectic were identified by Energy Dispersive X-Ray Spectroscopy (EDS).

Optical properties of Al_2O_3-$EuAlO_3$ eutectics were studied by absorption and luminescence spectroscopy at room temperature. The optical absorption of the eutectics was measured by transmission in transverse cross-sections obtained by polishing the samples down 200 μm in the 300-2600 nm range using a CARY 500 Scan from VARIAN spectrophotometer. Photoluminescence spectra were measured on the as-grown rod surface by exciting the samples with the light of a 1000 W tungsten lamp passed through a 0.22 m SPEX double monochromator. Fluorescence was detected at 90º through a 0.5 m Jarrell-Ash monochromator with a Hamamatsu R-928 photomultiplier.

3. RESULTS AND DISCUSSION

3.1. Microstructure

Figures 1(a), (b) and (c) show the SEM micrographs of the transverse cross sections of samples grown at 25, 350 and 750 mm/h, respectively. For all the samples a microstructure consisting of two phases, Al_2O_3 (dark phase) and $EuAlO_3$ (light phase), was observed. The microstructure was highly dependent on the growth rate, both the morphology and the size of the phases. For growth rates up to 100 mm/h the

microstructure was homogeneous throughout the entire cross-section of the grown rod. The microstructure consisted of an interpenetrated network of both phases (figure 1(a)). A slight elongation was observed along the growth direction in the longitudinal cross section. However, above 100 mm/h, regions consisting of $EuAlO_3$ fibers in an Al_2O_3 matrix coexisted with the interpenetrated pattern (figure 1(b)). At 750 mm/h, a cellular microstructure with only fibrilar domains was obtained (figure 1(c)).

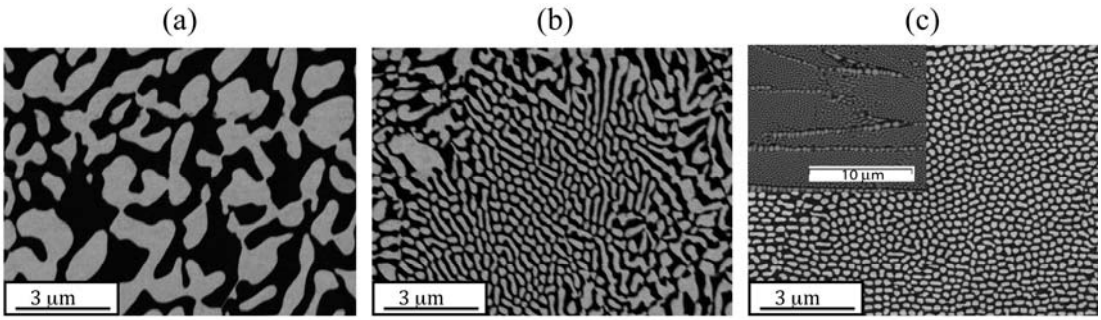

Figure 1: SEM transverse cross-sections of Al_2O_3-$EuAlO_3$ eutectic rods grown at (a) 100 mm/h, (b) 350mm/h and (c) 750 mm/h. $EuAlO_3$, light contrast, Al_2O_3, dark contrast.

The microstructure became finer when the growth rate increased. For the interpenetrated pattern, the phase size decreased from 1 μm in samples grown at 25 mm/h up to 250 nm in samples solidified at 350 mm/h. The interspacing length, λ, was measured using the interception linear methods in the SEM micrographs of the transverse sections. Figure 2 shows λ as a function of the growth rate. The dependence of λ with the solidification rate, V, could be fitted by the Hunt-Jackson law, $\lambda^2 V=C$ [14]. The C-value of 35 $\mu m^3/s$ was obtained for the Al_2O_3-$EuAlO_3$ eutectic from the fitting. This value is lower that those obtained for binary Al_2O_3-aluminum garnets eutectics [15] indicating that eutectics with perovskite structure phases tend to solidify with finer microstructures than those with garnet structures.

3.2. Optical absorption

The absorption spectra of eutectic rods were measured at room temperature. Figure 3 shows the absorption spectra for rods processed at 100 mm/h and 350 mm/h. The spectra were very similar for both growth rates, with a background absorption decreasing with λ^4 stronger in the sample grown at 350 mm/h. This structureless

absorption is due to light scattering at the eutectic interfaces and it increases as the microstructure is finer and therefore, the number of interfaces increases.

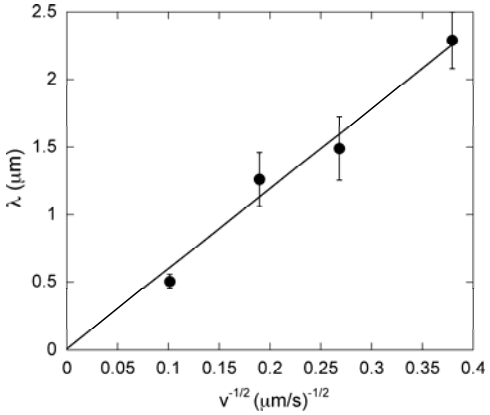

Figure 2: Dependence of the interspacing with the growth rate in the of Al_2O_3-$EuAlO_3$ eutectic rods. Circles correspond to the experimental values and the line is the fitting of the interpenetrated microstructure data to the Hunt-Jackson law with a C-value of 35 $\mu m^3 s^{-1}$.

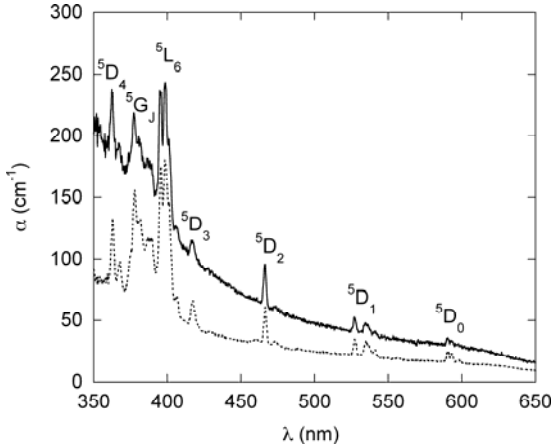

Figure 3: Visible optical absorption spectrum measured in Al_2O_3-$EuAlO_3$ eutectic rods grown at 100 mm/h (dotted line) and 350 mm/h (solid line) at room temperature.

Besides this Rayleigh scattering background, the spectrum consisted of groups of narrow lines that were attributed to the f–f optical excitations between the ground level and the excited states of the Eu^{3+} ($4f^6$) ion. The Eu^{3+} ground state corresponds to a $^7F_0$ energy level but the first excited energy level, $^7F_1$, is only at 360 cm^{-1} from the $^7F_0$ ground state [16] and so, it is thermally populated at room temperature. The remaining excited states in the ^7F manifold lie at energies higher than 1000 cm^{-1} and their population at room temperature can be neglected. In particular, the bands observed in the visible spectrum correspond to the absorption from the $^7F_0$ and $^7F_1$ states to the excited ^5D_J (J=1-4), $^5L_6$ and ^5G_J states whereas the infrared spectrum measures the transitions to the ^7F_J energy levels.

The intensity of the absorption is described by the "oscillator strengths" of the electronic transitions involved. The experimental oscillator strengths of the J→J' transitions, f_{EXP} ($J \rightarrow J'$), were obtained from the room-temperature area under the absorption bands as given by:

$$f_{EXP}(J \rightarrow J') = \frac{mc^2}{\pi e^2 N} \int \frac{\alpha(\lambda)}{\lambda^2} \, d\lambda \qquad (1)$$

m being the electron mass; *e*, the electron charge; *c*, the light velocity in vacuum; $\alpha(\lambda)$, the absorption coefficient and *N*, the number of Eu^{3+} ions per unit volume in the eutectic rod, and all the magnitudes are expressed in cgs units.

The Judd-Ofelt (J-O) theory [17,18] allows the calculation of the transition probabilities of 4f ions as a function of three parameters, Ω_2, Ω_4 and Ω_6,, the J-O parameters, using

$$f_{THEO}(J \rightarrow J') = \frac{8\pi^2 m \nu}{3h(2J+1)e^2 n^2}\left(\frac{n(n^2+2)^2}{9} S_{ED}(\Omega_2,\Omega_4,\Omega_6) + n^3 S_{MD}\right) \qquad (2)$$

S_{ED} and S_{MD} are the electric and magnetic dipole transitions probabilities, respectively with *n*, the refractive index. S_{ED} can be calculated using the double reduced unit tensor operator for Eu^{3+} [16] and the phenomenological intensity parameters Ω_2, Ω_4 and Ω_6,which are dependent of the host. S_{MD} is not affected by the ion local environment and it is taken as a constant for a given rare earth ion. By fitting the theoretical values of the transition oscillator strengths to the experimental ones derived from the optical absorption spectra, the J-O intensity parameters could be obtained. In order to calculate the J-O parameters, it is necessary to know in which eutectic phase enters the Eu^{3+} ion. Trivalent rare earth ions can be present in β-Al_2O_3. However, in the case of Al_2O_3-Eu_2O_3 system, from the experimental phase diagram [12] and previous X-ray diffraction studies [11], it is clearly stated that the only eutectic phases are α-Al_2O_3 and $EuAlO_3$. Therefore, Eu^{3+} was assumed to be present only in the $EuAlO_3$ phase as the europium content in α-Al_2O_3 is expected to be negligible. A refraction index n=2 was taken in the calculations [19]. The thermal population of the $^7F_0$ and $^7F_1$ ground states at room temperature, 0.66 and 0.34, respectively, was taken into account in the calculations. The intensity parameter values were Ω_2=18.3x10^{-20} cm^2; Ω_4=25.8x10^{-20} cm^2 and Ω_6=8.8x10^{-20} cm^2 for samples grown at 100 mm/h and Ω_2=18.1x10^{-20} cm^2; Ω_4=33.4x10^{-20} cm^2 and Ω_6=8.5x10^{-20} cm^2 for those processed at 350 mm/h, very similar for both growth rates.

3.3 Photoluminescence

Photoluminescence was measured at room temperature in samples grown at 100 and 350 mm/h. Figure 4 shows the emission spectra of both samples when excited at 396 nm with broad bandwidth. In both cases, the emission spectra showed narrow lines

which consisted of two main emission bands centred at 595 nm and 616 nm. The excitation spectrum of the 616 nm emission (inset in figure 4) shows similar features to those found in the absorption spectrum, allowing attributing the emission to the trivalent europium 4f-transitions. The maximum in emission was obtained for an excitation wavelength of 396 nm, which corresponds to the more intense Eu^{3+} absorption line. Intense light emission was only observed from the $^5D_0$ energy level to the lower ^7F_J levels as the ^5D_J (with J>0) levels were non-radiatively depopulated to the $^5D_0$ emitting level. Therefore, the 595 nm and 616 nm luminescence bands were assigned to the $^5D_0 \rightarrow {}^7F_1$ and $^5D_0 \rightarrow {}^7F_2$ transitions of Eu^{3+} ion, respectively. An intense emission at 700 nm prevented us from identifying clearly lower energy transitions corresponding to the relaxation to $^7F_3$ or $^7F_4$ energy levels. Excitation spectrum allowed attributing this emission to Cr^{3+} ions in the α-alumina phaseCr^{3+} is an impurity in the Al_2O_3 raw powders, present in small amounts at the level of traces of few ppm. As a consequence, the effect of Cr^{3+} in the microstructure and absorption was negligible. However, the strong efficiency in the R-line luminescence of Cr^{3+} added to the strong concentration quenching in the Eu^{3+} luminescence allowed the Cr^{3+} emission to be observed.

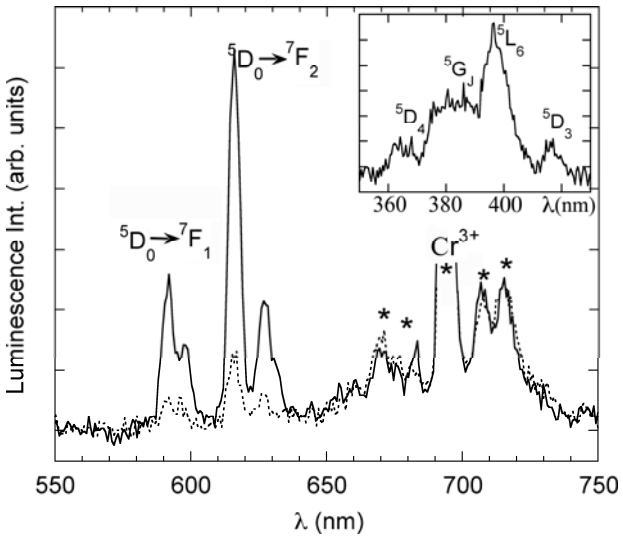

Figure 4: Photoluminescence spectrum measured in Al_2O_3-$EuAlO_3$ eutectic rods grown at 100 mm/h (dotted line) and 350 mm/h (solid line) at room temperature when excited at 396 nm. Inset: Excitation spectrum of the 616 nm emission.

As observed in figure 4, the $^5D_0 \rightarrow {}^7F_1$ magnetic dipole allowed transition is weaker than that of the $^5D_0 \rightarrow {}^7F_2$ electric dipole transition. The $^5D_0 \rightarrow {}^7F_2$ is a hypersensitive

transition, that is, depends strongly on the Eu^{3+} local environment [20], showing a higher intensity in non-centrosymmetric sites. In our host, the relative intensity is found to be high, as corresponds to the europium site in the orthorrhombic perovskite [21], without inversion symmetry in the A-site.

The Eu^{3+} luminescence appears more intense in samples grown at 350 mm/h. We should note that since europium is a constituent ion, strong concentration quenching of luminescence takes place. That is the reason for the weak luminescence observed in samples grown at 100 mm/h. However, in samples solidified at higher growth rates, the emission increases significantly, probably due to the microstructure refinement. At this growth rates the size of $EuAlO_3$, the only phase containing Eu^{3+}, decreases down 250 nm or less and there are an increasing number of Eu^{3+} ions closer to the Al_2O_3 phase where transfer between Eu^{3+} ions is hindered, explaining the lower concentration quenching in the sample with the finer microstructure.

4. CONCLUSIONS

Al_2O_3-$EuAlO_3$ eutectic rods were grown from the melt by using the LHFZ method. The influence of the growth rate in the microstructure and optical properties was investigated. Microstructure became finer with the growth rate, the interspacing following the Hunt-Jackson law. Homogeneous interpenetrated microstructure was only obtained at lower growth rates. Red fluorescence was obtained at 616 nm from Eu^{3+} ions in the perovskite phase. The observed luminescence was sensibly stronger in samples grown at 350 mm/h than at 100 mm/h, most probably due to smaller concentration quenching associated to the refinement of the microstructure.

ACKNOWLEDGEMENTS

The authors acknowledge the financial support from the Ministerio de Ciencia e Innovación de España and from the FEDER founds of the EC under project MAT2009-13979-C03-03, and from the European Community under project ENSEMBLE NMP4-SL-2008-213669. Authors acknowledge the use of Servicio de Microscopia Electrónica (Servicios de Apoyo a la Investigación), Universidad de Zaragoza. M. C. Mesa thanks the Gobierno de Aragón for a grant.

REFERENCES

[1] J. LLorca and V. M. Orera, Prog. Mater. Sci. 51 (6) (2006) 711-809.

[2] Y. Waku, S. Sakata, A. Mitani, Shimizu K, M. Hasebe, J. Mat. Sci. 37 (2002) 2975.

[3] L. E. Matson, N. Hecht, J. Eur. Ceram. Soc. 19 (1999) 2487-2501.

[4] J. Y. Pastor, J. Llorca, A. Salazar, P. B. Oliete, I. de Francisco, J. I. Peña, J. Am. Ceram. Soc. 88 (2005) 1488-1495.

[5] V. M. Orera, J. I. Peña, R. I. Merino, J. A: Lázaro, J. A. Vallés and M. A. Rebolledo, Appl. Phys. Lett. 71 (1997) 2746.

[6] R.I. Merino, J.A. Pardo, J.I. Peña, V.M. Orera, Appl.Phys. Lett. 88 (2002) 589-591.

[7] N. Nakagawa, H. Ohtsubo, Y. Waku, H. Yugami, J. Eur. Ceram. Soc. 25 (2005) 1285-1291.

[8] M. Dejneka, E. Snitzer, R. E. Riman, J. Lumin. 65 (1995) 227-245.

[9] C. Louis et al, J. Crys. Growth 265 (2004) 459-465.

[10] L. Mazerolles, L. Perriere, S. Lartigue-Korinek, N. Piquet, M. Parlier, J. Eur. Ceram. Soc. 28 (2008) 2301-2308.

[11] A. Yoshikawa, K. Hasegawa, J. H. Lee, S. D. Durbin, B. M. Epelbaum, D. H. Yoon, T. Fukuda, Y. Waku, J. Cryst. Growth 218 (2000) 67-73

[12] M. Mizuno, T. Yamada and T. Noguchi, 85 Yogyo-Kyokai-Shi (1977) 543-548.

[13] P. B. Oliete, J. I. Peña, J. Cryst. Growth 304 (2007) 514-519.

[14] K. A. Jackson, J. D. Hunt, Trans. Metal. Soc. AIME 236 (1966) 1129-1142.

[15] M. C. Mesa, P. B. Oliete, V. M. Orera, J. Y. Pastor, A. Martín, J. LLorca, J. Eur. Ceram. Soc. 31 (2011), 1241-1250.

[16] W. T. Carnall, P. R. Fields, K. Rajnak, J. Chem. Phys. 49 (1968) 4450-4455.

[17] B. R. Judd, Phys. Rev. 127 (1962) 750-761.

[18] G. S. Ofelt, J. Chem. Phys. 37 (1962) 511-520.

[19] J. D. Bass, Phys. Earth Planet. Int. 36 (1984) 145-156.

[20] N. Rakov, G. S. Maciel, J. Lumin. 127 (2007) 703-706.

[21] A. Kumar, A. S. Verma, J. Alloys Compound 480 (2009) 650-657.